Computational Geosciences **7:** 253–273, 2003.

Generalized coarse graining procedures for flow in porous media

Sabine Attinger *
Institute of Hydromechanics and Water Resources Management (IHW), Swiss Federal Institute of Technology (ETH), Zurich, Switzerland
E-mail: attinger@ihw.baug.ethz.ch

Received January 2002; accepted 14 October 2002

This paper focuses on heterogeneous soil conductivities and on the impact their resolution has on a solution of the piezometric head equation: owing to spatial variations of the conductivity, the flow properties at larger scales differ from those found for experiments performed at smaller scales. The method of coarse graining is proposed in order to upscale the piezometric head equation on arbitrary intermediate scales. At intermediate scales large scale fluctuations of the conductivities are resolved, whereas small scale fluctuations are smoothed by a partialy spatial filtering procedure. The filtering procedure is performed in Fourier space with the aid of a low-frequency cut-off function. We derive the partially upscaled head equations. In these equations, the impact of the small scale variability is modeled by scale dependent effective conductivities which are determined by additional differential equations. Explicit results for the scale dependent conductivity values are presented in lowest order perturbation theory. The perturbation theory contributions are summed up with using a renormalisation group analysis yielding explicit results for the effective conductivity in isotropic media. Therefore, the results are also valid for highly heterogeneous media. The results are compared with numerical simulations performed by Dykaar and Kitanidis (1992). The method of coarse graining combined by a renormalisation group analysis offers a tool to derive exact and explicit expressions for resolution dependent conductivity values. It is, e.g., relevant for the interpretation of measurement data on different scales and for reduction of grid-block resolution in numerical modeling.

Keywords: coarse graining, filtering procedures, flow, heterogeneous porous media, multi-scale modelling

1. Introduction

Measurement results of soil properties which are spatially variable crucially depend on the resolution scale at which they are resolved. This paper focuses on heterogeneous soil conductivities and on the impact their resolution has on the piezometric head equation. The need to know how the head equation depends on its resolution scale become

* Currently at: Computational Laboratory (Colab), Swiss Federal Institute of Technology (ETH), Zurich, Switzerland.

most apparent when constructing numerical models with coarser resolution. Upscaling methods can be used in order to incorporate subgrid-scale information into the model parameter estimation of a model with coarser resolution.

In many practical problems, the analysist has data consisting of local measurements across the site and several field tests. At small scale, soil conductivities are, e.g., measured by core sampling: small unperturbed cores with a typical diameter of about 10 cm are taken and small scale flow experiments are performed on them. The measurement gives local porosity and conductivity values, which typically differ from core to core location. A heterogeneous porosity and conductivity distribution results with a typical measurement resolution of about 10 cm. By interpretation of the data, mean values, variances and covariances can be identified. Prominent examples are the Borden Test site (1986) or the Cap Cod Test site (1992) where core samples were tested in a lab permeameter and statistical properties of the conductivity were derived.

At larger scales, e.g., in-situ pumping tests are performed. Short time pumping tests of wells provide information on the vicinity of a well (meter scale). Within these experiments draw-downs and fluxes are measured and short-range conductivities are identified via Darcy's law. In contrast, long time pumping tests characterize the medium on a more regional scale (scale of hundreds of meters) and a long-range or effective conductivity is measured. These are only some examples of conductivity measurements of a soil at different scales. However, all experiments have in common that they average information over a volume determined by the resolution scale of the measurement procedure. The influence of the spatial average of the conductivity data by using different measurement techniques has been discussed, e.g., by Gelhar [16], Journel and Huijbregts [22] or Vanmarcke [33]. A summary of conductivity data from different field sites can be found, e.g., in [17]. Therefore, it is useful for the practioneer to have insight into how data collected at different scales are related to each other. In the groundwater literature, spatial filters are widely used to conceptually represent measurements of conductivities on different scales, for further reference see, e.g., also [3,11,18,26]. A detailed discussion of their work can be found in [5].

The derivation of large scale effective parameters has been done, e.g., in the framework of stochastic theories. Mean piezometric heads are determined by averaging the head equation over many realizations of different conductivity fields. The mean heads are characterized by effective conductivity values. Approximate results are derived in lowest order perturbation theory of the variance of the logarithm of the conductivity. For further reference see, e.g., [7,17]. Higher order perturbation theory contributions to the effective conductivity were, e.g., calculated by Dean et al. [8]. On the other hand, exact expressions for the effective conductivities can been found in the work of Neuman et al. [24]. They developed an exact nonlocal formalism for the determination of effective conductivity values. However, for the evaluation of their expressions they have to calculate them numerically in a so-called localisation approximation. Moreover, effective conductivity values may be determined as well by volume averaging methods or homogenization theory techniques, see, e.g., [34] or [27]. In these approaches, an effective head equation is derived. Effective conductivity values are obtained from the solution of an additional differential equation. In the limit of small fluctuations the results reduce to the standard perturbation theory results cited above.

However as mentioned above, for the consistent interpretation of measurements performed at different resolution scales, one is more interested in averaging the head equation on intermediate scales than on very large scales. Numerical investigations have been performed, e.g., by Hou et al. [20], Nilsen and Espendal [25], Efendiev et al. [15] or Durlovsky [12]. Analytical investigations are only found for a radial flow configuration. Desbarats [10] developed a semianalytical formula for an equivalent scale dependent conductivity. Sanchez-Vila [31], Sanchez-Vila et al. [32] and Indelman et al. [21] derived analytical expressions for the equivalent conductivity in a radially convergent flow field. They found that it equals the arithmetic mean in the vicinity of the well but approaches the geometric mean in the far field of the well.

This paper presents a systematic approach to derive a resolution-dependent head equation where small scale heterogeneities up to an arbitrary length scale are filtered out and large scale heterogeneities are still resolved. For this purpose, we choose a method called coarse graining. Basically, it is a partial volume averaging procedure originally developed in the context of large eddy simulation in turbulent flow, for further reference see also [23]. The method was also applied by Dykaar and Kitanidis [13] for the numerical determination of the effective hydraulic conductivity. Moreover, Beckie et al. [6] have used the method for spatial filtering of the head equation. They derived spatially filtered head equations in small perturbation assumption.

We overcome these limitations and derive spatially filtered head equations that are exact. In general, they are nonlocal. However, for further mathematical treatment we localise them and approximate the subscale effects by their ensemble mean. Iteration of the filtering procedure over stepwise coarser averaging volumes allows to formulate the coarse graining procedure in terms of a differential equation which becomes a renormalisation group equation.

The novelty of our results is that we present explicit results for resolution dependent model parameters of the spatially filtered head equation that are free from small perturbation assumptions.

In section 2, we introduce the flow model and explain the concept of coarse graining. It is applied to spatially filter the heterogeneous head equation in section 3. Explicit results are derived in section 4 in lowest order perturbation theory first. We extend our perturbation theory results to any order perturbation theory by using renormalisation group analysis in section 5. In section 6, we present a numerical model that tests the spatially filtered head equation for its physical plausibility. We conclude with a discussion.

2. The concept of coarse graining

The steady-state head distribution for single-phase, incompressible flow through a heterogeneous medium is described by

$$-\nabla K(\mathbf{x})\nabla\phi(\mathbf{x}) = \rho(\mathbf{x}), \tag{1}$$

where $\phi(\mathbf{x})$ is the pressure or piezometric head distribution, $K(\mathbf{x})$ a local conductivity field and $\rho(\mathbf{x})$ represents source or sink terms. For simplicity, we choose boundaries at infinity. However, it is possible to extend the formalism presented in this paper to more general situations.

The hydraulic conductivity K is a spatially heterogeneous field which is modelled as lognormally distributed in space

$$K(\mathbf{x}) = K_0 \exp\bigl(f(\mathbf{x})\bigr), \tag{2}$$

where $f(\mathbf{x})$ is spatially normal distributed. K_0 is a hydraulic conductivity of value one that gives K the correct dimension. We split $\log K$ into its mean value and the deviation from that value

$$f(\mathbf{x}) = \overline{f} + \tilde{f}(\mathbf{x}). \tag{3}$$

The overbar $\overline{(\ldots)}$ denotes an ensemble average over the normal distribution of $f(\mathbf{x})$. By construction, the ensemble average of the fluctuating part vanishes, $\overline{\tilde{f}(\mathbf{x})} = 0$. Assuming a stationary distribution for $f(\mathbf{x})$, the correlation function $w(\mathbf{x}, \mathbf{x}') \equiv \overline{\tilde{f}(\mathbf{x})\tilde{f}(\mathbf{x}')}$ only depends on the distance, $w(\mathbf{x} - \mathbf{x}')$. For mathematical reasons, we choose for the correlation function a Gaussian

$$w(\mathbf{x} - \mathbf{x}') \equiv \sigma_f^2 \exp\left(-\frac{(\mathbf{x} - \mathbf{x}')^2}{2l_0^2}\right), \tag{4}$$

where σ_f^2 is the variance and l_0 an isotropic correlation length. For anisotropically distributed $\log K$ fields, the correlations are characterized in each spatial direction by a different correlation length l_i for $i = 1, \ldots, d$ and d is the spatial dimension of the flow problem.

The head equation (1) and the statistical properties of the heterogeneous hydraulic conductivity field are valid on a scale which is at least of the order of magnitude of a representative pore volume for which Darcy's law holds. In the following we will refer to this scale as the local scale. In standard or global upscaling procedures, all hydraulic conductivity fluctuations are averaged out and replaced by an effective hydraulic conductivity tensor. In contrast to that, the central focus of this paper is to introduce and apply the concept of a partially spatial averaging procedure called coarse graining. Coarse graining procedures aim at coarsening the heads to intermediate scales by averaging the heads over so-called filter volumes of intermediate sizes. In the following, we assume that the coarse scale is characterized by a typical length λ and demonstrate the concept of the coarse graining on the local head field $\phi(\mathbf{x})$.

Definition (Coarse graining in real space). Fluctuations of $\phi(\mathbf{x})$ are smoothed out over a filter volume λ^d around the location $\mathbf{x}$ by

$$\bigl\langle \phi(\mathbf{x}) \bigr\rangle_\lambda \equiv \frac{1}{\lambda^d} \int_{-\lambda/2}^{+\lambda/2} \mathrm{d}^d x' \phi(\mathbf{x} + \mathbf{x}'), \tag{5}$$

where $\langle\phi(\mathbf{x})\rangle_\lambda$ is the coarser head distribution, d the spatial dimension and $\mathrm{d}^d x$ an infinitesimal volume element.

For further mathematical treatment, we define the Fourier transform of the head field,

$$\phi(\mathbf{x}) \equiv \int \mathrm{d}^d q \exp(\mathrm{i}\mathbf{q}\mathbf{x})\phi(\mathbf{q}), \tag{6}$$

where $\mathrm{d}^d q$ denotes $1/(2\pi)^d \int \mathrm{d}^d q$, for the sake of brevity. Using its Fourier transform the partial volume average of the head field (5) can be written as

$$\begin{aligned}\langle\phi(\mathbf{x})\rangle_\lambda &= \frac{1}{\lambda^d}\int_{-\lambda/2}^{+\lambda/2} \mathrm{d}^d x' \int \mathrm{d}^d q \exp\bigl(-\mathrm{i}\mathbf{q}(\mathbf{x}+\mathbf{x}')\bigr)\phi(\mathbf{q}) \\ &= \int \mathrm{d}^d q \exp(-\mathrm{i}\mathbf{q}\mathbf{x}) \prod_i \frac{\sin(q_i\lambda/2)}{q_i\lambda/2}\phi(\mathbf{q}).\end{aligned} \tag{7}$$

Here q_i is ith the component of the Fourier vector $\mathbf{q}$. Small q-values contribute to the integrals in (7) whereas large q-values are suppressed by the fast oscillations of the sine-functions for large q-values. In other words, the sine-functions act as filter functions for q-values: the larger λ the wider is the spectrum of q-values which are filtered out. Therefore, the coarse graining procedure can be also considered as follows:

Definition (Coarse graining in Fourier space). The head field is transformed into Fourier space, q-values larger than a cut-off value λ^{-1} are filtered out and the function is transformed back to real space. We define this filter process in Fourier space by means of a projection onto small wave numbers

$$\phi(\mathbf{q}_-) \equiv \begin{cases} \phi(\mathbf{q}) & \text{if } q_i < \dfrac{1}{\lambda}, \\ 0 & \text{otherwise.}\end{cases}$$

Thus, the Fourier transform of a local head field is composed of its projection on small q-values and the complementary projection on large q-values,

$$\phi(\mathbf{q}) = \phi(\mathbf{q}_-) + \phi(\mathbf{q}_+). \tag{8}$$

3. Coarse graining of the head equation

The equivalence of filtering in Fourier space can be employed for coarse graining the head equation. We will give here only a brief review of the different steps of the coarse graining method that was originally developed for large eddy-simulations in fluid mechanics. For further reference the reader is referred to [23].

Step 1. Fourier transformation of the head equation

$$-\overline{K}\mathbf{q}^2\phi(\mathbf{q}) + (\mathrm{i}\mathbf{q})\int \mathrm{d}^d q'\,\widetilde{K}(\mathbf{q}-\mathbf{q}')\,(\mathrm{i}\mathbf{q}')\phi(\mathbf{q}') = -\rho(\mathbf{q}). \tag{9}$$

Using the Green's function formalism, the solution for Fourier transformed heads can be written as

$$\phi(\mathbf{q}) = -G^0(\mathbf{q})\rho(\mathbf{q}) - G^0(\mathbf{q})(\mathrm{i}\mathbf{q})\int \mathrm{d}^d q'\,\widetilde{K}(\mathbf{q}-\mathbf{q}')(\mathrm{i}\mathbf{q}')\phi(\mathbf{q}'), \tag{10}$$

where $G^0(\mathbf{q})$ is the Green's function of the homogeneous head equation (with fluctuations of hydraulic conductivity set to zero, $\widetilde{K} = 0$). It solves $-\overline{K}\mathbf{q}^2 G^0(\mathbf{q}) = 1$ and is therefore given by $G^0(\mathbf{q}) = -1/(\overline{K}\mathbf{q}^2)$.

For shorter notation, we introduce the operators $L_{q,q'}$ and $R_{q,q'}$ by

$$L_{q,q'}\phi(\mathbf{q}') \equiv -\overline{K}\,\mathbf{q}^2\phi(\mathbf{q}) + (\mathrm{i}\mathbf{q})\int \mathrm{d}^d q'\,\widetilde{K}(\mathbf{q}-\mathbf{q}')(\mathrm{i}\mathbf{q}')\phi(\mathbf{q}'), \tag{11}$$

$$R_{q,q'}\phi(\mathbf{q}') \equiv \mathrm{i}\mathbf{q}\int \mathrm{d}^d q'\,\widetilde{K}(\mathbf{q}-\mathbf{q}')(\mathrm{i}\mathbf{q}')\phi(\mathbf{q}'). \tag{12}$$

The operator notation allows to write equations (9) and (10) in very compact form:

$$L_{q,q'}\phi(\mathbf{q}') = -\rho(\mathbf{q}), \tag{13}$$

$$\phi(\mathbf{q}) = -G^0(\mathbf{q})\rho(\mathbf{q}) - G^0(\mathbf{q})R_{q,q'}\phi(\mathbf{q}'). \tag{14}$$

We assume that the inverse operator $L^{-1}_{q,q'}$ exists, too. It is defined by

$$L^{-1}_{q,q''}L_{q'',q'} \equiv \delta_{q,q'}. \tag{15}$$

It implies that $L^{-1}_{q,q'}$ is related to the Fourier transformed Green's function of the full head equation by

$$L^{-1}_{q,q'} = G_{q,-q'}. \tag{16}$$

Note that a minus sign in the Green's function arises. The Green's function in real space is the solution of the full head equation assuming Delta functions $\delta(\mathbf{x}-\mathbf{x}')$ as source terms. Transforming the governing equation into Fourier space, we get $\delta(\mathbf{q}+\mathbf{q}')$ as source terms which differ from the right-hand side of (15) by a minus sign.

Step 2. Applying the filtering procedure to the heads provides the following set of equations

$$\begin{aligned}\phi(\mathbf{q}_-) &= -G^0(\mathbf{q}_-)\rho(\mathbf{q}_-) - G^0(\mathbf{q}_-)R_{q_-,q'}\phi(\mathbf{q}') \\ &= -G^0(\mathbf{q}_-)\rho(\mathbf{q}_-) - G^0(\mathbf{q}_-)R_{q_-,q'_+}\phi(\mathbf{q}'_+) - G^0(\mathbf{q}_-)R_{q_-,q'_-}\phi(\mathbf{q}'_-),\end{aligned} \tag{17}$$

$$\begin{aligned}\phi(\mathbf{q}_+) &= -G^0(\mathbf{q}_+)\rho(\mathbf{q}_+) - G^0(\mathbf{q}_+)R_{q_+,q'}\phi(\mathbf{q}') \\ &= -G^0(\mathbf{q}_+)\rho(\mathbf{q}_+) - G^0(\mathbf{q}_+)R_{q_+,q'_+}\phi(\mathbf{q}'_+) - G^0(\mathbf{q}_+)R_{q_+,q'_-}\phi(\mathbf{q}'_-).\end{aligned} \tag{18}$$

Due to the filter the inner integration variables $\mathbf{q}'$, $\mathbf{q}''$ and $\mathbf{q}'''$ are restricted to large, respectively small wave numbers. The arguments of the functions and the operators are also defined on the restricted wave number spectra. Both equations are coupled because the heads on the right-hand sides still depend on long as well as on short wave number contributions. As pointed out above, the main interest is in $\phi(\mathbf{q}_-)$ because its Fourier back transform is the coarse grained head distribution we want to determine. To that end, the solution for $\phi(\mathbf{q}_+)$ is inserted into the equation for $\phi(\mathbf{q}_-)$.

Step 3. Decoupling of the filtered heads. We solve the implicit set of equations (17) and (18) by making use of the inverse operator as introduced in step 1 but with restricted wave spectra:

$$\phi(\mathbf{q}_+) = -L^{-1}_{q_+,q'_+}\rho(\mathbf{q}_+) - L^{-1}_{q_+,q'_+}R_{q'_+,q''_-}\phi(\mathbf{q}''_-), \tag{19}$$

$$\phi(\mathbf{q}_-) = -L^{-1}_{q_-,q'_-}\rho(\mathbf{q}_-) - L^{-1}_{q_-,q'_-}R_{q'_-,q''_+}\phi(\mathbf{q}''_+). \tag{20}$$

The remaining step is simple. We have to insert $\phi(\mathbf{q}_+)$ into (20) and get

$$\phi(\mathbf{q}_-) = -L^{-1}_{q_-,q'_-}\rho(\mathbf{q}_-) - L^{-1}_{q_-,q'_-}R_{q'_-,q''_+}\big(-L^{-1}_{q''_+,q'''_+}\rho(\mathbf{q}'''_+) - L^{-1}_{q''_+,q'''_+}R_{q'''_+,q''''_-}\phi(\mathbf{q}''''_-)\big). \tag{21}$$

Step 4. Mean field approximation and Localisation approximation. We rewrite (21) into

$$L_{q_-,q'_-}\phi(\mathbf{q}'_-) = -\rho(\mathbf{q}_-) - R_{q_-,q'_+}\big(-L^{-1}_{q'_+,q''_+}\rho(\mathbf{q}''_+) - L^{-1}_{q'_+,q''_+}R_{q''_+,q'''_-}\phi(\mathbf{q}'''_-)\big). \tag{22}$$

By its structure, (22) looks already like the filtered head equation we are aiming for. The left-hand side of the equation is equivalent to equation (9) with all Fourier variables restricted to small wave numbers. The large wave fluctuations show their impact by means of the second and third terms on the right-hand side. For further mathematical treatment, we approximate the long wave fluctuations by their ensemble mean values (mean field approximation) and, therefore, the second term on the right-hand side vanishes. This can be seen easily when expanding L^{-1} in a perturbation series and performing the ensemble average term by term: the statistical translation invariance of the hydraulic conductivity field requires that $\mathbf{q} + \mathbf{q}'' = 0$ with $q > \lambda^{-1}$ and $q'' < \lambda^{-1}$ which cannot be fulfilled simultaneously and the terms have to vanish.

The third term on the right-hand side does not vanish. Writing the term explicitly, we find

$$\begin{aligned}&\mathbf{iq}_-\int \mathrm{d}^d q'_+\mathrm{d}^d q''_+\overline{\widetilde{K}(\mathbf{q}_+ - \mathbf{q}'_+)\,\mathbf{i}\mathbf{q}'_+G(\mathbf{q}'_+, -\mathbf{q}''_+)\,\mathbf{i}\mathbf{q}''_+\widetilde{K}(\mathbf{q}''_+ - \mathbf{q}_-)}\,\mathbf{iq}_-\phi(\mathbf{q}_-)\\ &\quad\equiv \mathbf{iq}_-\delta\mathbf{K}^{\mathrm{eff}}(\mathbf{q}_-,\lambda)\,\mathbf{iq}_-\phi(\mathbf{k}_-).\end{aligned} \tag{23}$$

$\delta\mathbf{K}^{\mathrm{eff}}(\mathbf{q}_-,\lambda)$ can be understood as a scale-dependent effective hydraulic conductivity tensor which is induced by small scale heterogeneities varying on typical length scales smaller than λ. Note that the Fourier-back-transform of (23) yields a nonlocal, resolution dependent hydraulic conductivity tensor as found as well by Neuman and

Orr [24]. However, we simplify (23) by evaluating $\delta\mathbf{K}^{\text{eff}}(\mathbf{q},\lambda)$ at $\mathbf{q}=0$ which corresponds to localisation in the work of Neumann and Orr [24].

Step 5. Fourier backtransformation. In real space, equation (23) reads after localisation

$$-\nabla\big(\overline{K}+\langle\widetilde{K}(\mathbf{x})\rangle_\lambda\big)\nabla\langle\phi(\mathbf{x})\rangle_\lambda+\nabla\delta\mathbf{K}^{\text{eff}}(\mathbf{q}=0,\lambda)\nabla\langle\phi(\mathbf{x})\rangle_\lambda=\langle\rho(\mathbf{x})\rangle_\lambda. \tag{24}$$

4. Explicit results in lowest order perturbation theory for isotropic media

Explicit results for $\delta K^{\text{eff}}(\lambda)$ can be found in lowest order perturbation theory for weakly heterogeneous hydraulic conductivity fields. In this approximation, the full Green's function (16) reduces to the Green's function of the homogeneous head equation. In isotropic media, the effective hydraulic conductivity tensor simplifies to a diagonal tensor with identical entries. They are given as the solution of the following integrals

$$\delta\mathbf{K}^{\text{eff}}_{ij}(\lambda)=-\delta_{ij}\overline{K}\sigma_f^2\int \mathrm{d}^d q'_+\exp\left(-\frac{\mathbf{q}'^2 l_0^2}{2}\right)\frac{q'_i q'_j}{\mathbf{q}'^2}\frac{(2\pi l_0^2)^{d/2}}{(2\pi)^d}. \tag{25}$$

For further mathematical treatment, we relax this constraint and replace it by the smoother cut-off function

$$1-\exp\left(-\frac{\mathbf{q}'^2\lambda^2}{8}\right). \tag{26}$$

We choose the width of the Gaussian function such that its Gaussian Fourier back transform has a similar width as the sharp cut-off function defined in the partial spatial average (5). (25) with the smooth cut-off function (26) yields isotropic conductivities values

$$\delta K^{\text{eff}}(\lambda)=-\overline{K}\sigma_f^2\frac{1}{d}\left(1-\left(\frac{l_0^2}{l_0^2+\lambda^2/4}\right)^{d/2}\right) \tag{27}$$

for spatial dimensions $d=1,2$ or 3. Equation (27) combined with the arithmetic mean $\overline{K}$ expanded in powers of σ_f^2 produces a mean coarse grained hydraulic conductivity of

$$K_g\left(1+\sigma_f^2\frac{1}{2}-\sigma_f^2\frac{1}{d}\left(1-\left(\frac{l_0^2}{l_0^2+\lambda^2/4}\right)^{d/2}\right)\right). \tag{28}$$

In the limit of zero coarse graining, all fluctuations of the hydraulic conductivity are modelled explicitly and λ is zero. In this case, the mean hydraulic conductivity value is accordingly given by the arithmetic mean or in lowest order perturbation theory by $K_g(1+\sigma_f^2/2+\cdots)$. The fluctuating part of the hydraulic conductivity is equivalent to the full fluctuations, $\langle\widetilde{K}(\mathbf{x})\rangle_{\lambda=0}\equiv\widetilde{K}(\mathbf{x})$, as in the local equation (1). In the other limiting case of coarse graining over very large volumes, λ is much larger than the correlation length l_0 and the mean hydraulic conductivity has to be equivalent, e.g., in two

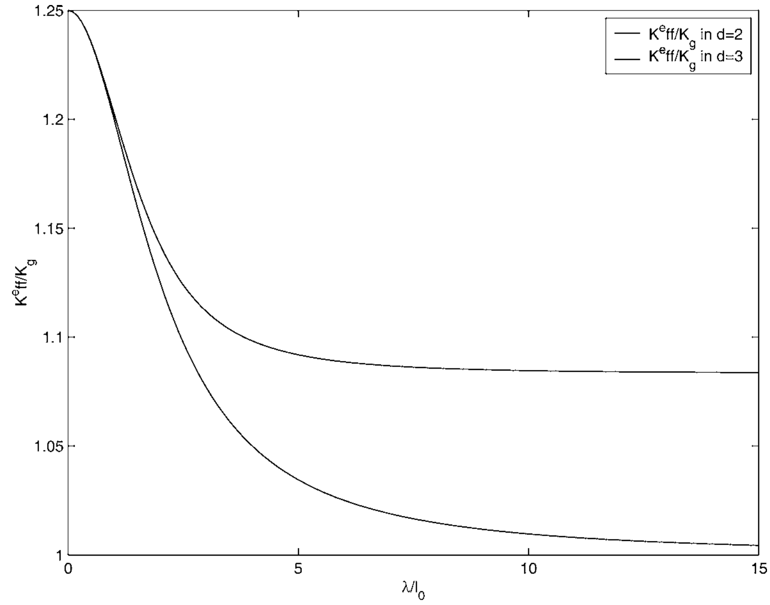

Figure 1. K^{eff}/K_g in lowest order perturbation theory for two and three spatial dimensions with $\sigma_f^2 = 0.5$.

dimensions to the geometric mean. Equation (28) is consistent with this result. The fluctuating part $\langle \widetilde{K}(\mathbf{x}) \rangle_{\lambda \gg l_0}$ vanishes simply because it is equivalent to the volume average of $\widetilde{K}(\mathbf{x})$ over a representative part of the medium containing many correlation lengths. This average value is zero by definition. On intermediate scales equation (28) interpolates between the arithmetic mean and the effective hydraulic conductivity value. The full behavior of $K^{\mathrm{eff}}(\lambda)$ can be seen in figure 1 where it is plotted against the dimensionless quantity λ / l_0.

4.1. Statistical properties of the coarse grained hydraulic conductivity fluctuations

Next, we present the statistical properties of the hydraulic conductivity field fluctuating on coarser scales $\langle \widetilde{K}(\mathbf{x}) \rangle_\lambda$. Explicitly, it is written as

$$\langle \widetilde{K}(\mathbf{x}) \rangle_\lambda \equiv \frac{1}{\lambda^d} \int_{-\lambda/2}^{+\lambda/2} \mathrm{d}^d x' \, \widetilde{K}(\mathbf{x} + \mathbf{x}'). \tag{29}$$

Obviously, its mean value vanishes because the statistical and the spatial average are interchangeable which leads to $\overline{\langle \widetilde{K}(\mathbf{x}) \rangle_\lambda} = 0$. The correlation function of the hydraulic conductivity field at coarser scales follows as

$$\begin{aligned} \overline{\langle \widetilde{K}(\mathbf{x}) \rangle_\lambda \langle \widetilde{K}(\mathbf{x}) \rangle_\lambda} &\equiv \int \mathrm{d}^d q \, \mathrm{d}^d q' \exp(\mathrm{i}\mathbf{q}\mathbf{x} + \mathrm{i}\mathbf{q}'\mathbf{x}) \overline{\widetilde{K}(\mathbf{q}) \widetilde{K}(-\mathbf{q})} \delta(\mathbf{q} + \mathbf{q}') \exp\left(-\frac{q^2 \lambda^2}{8}\right) \\ &= \sigma_f^2 \left(\frac{l_0^2}{l_0^2 + \lambda^2/4}\right) \exp\left(-\frac{(\mathbf{q} - q')^2}{l_0^2 + \lambda^2/4}\right) \end{aligned} \tag{30}$$

which leads to a hydraulic conductivity variance on coarser scales of

$$\sigma_f^2(\lambda) \equiv \sigma_f^2 \left(\frac{l_0^2}{l_0^2 + \lambda^2/4} \right)^{d/2}. \tag{31}$$

If all hydraulic conductivity fluctuations are resolved explicitly and no coarse graining procedure has been applied, λ is zero and the variance reduces to the small scale variance as introduced in section 2. On the other hand, if all hydraulic conductivity fluctuations are averaged out and replaced by an effective hydraulic conductivity tensor, the ratio λ / l_0 becomes very large and the variance very small. The variance approaches zero in the limit of $\lambda / l_0 \to \infty$, which is equivalent to a global upscaling of the hydraulic conductivity without intermediate coarse graining. This result is consistent with field data reviewed by Gelhar [17]. In general, three dimensionally resolved hydraulic conductivity data show a higher variance than depth-averaged data. A similar result was found by Stauffer [28]. He analyzed the statistical properties of conductivities averaged over vertical profiles.

In contrast, the correlation length of the coarse grained logarithmic hydraulic conductivity fluctuations is increased compared with the small scale correlation length. From (30) the corresponding correlation length can be identified as

$$l_\lambda = \left(l_0^2 + \frac{\lambda^2}{4} \right)^{1/2}. \tag{32}$$

By construction, the resolution scale of coarse grained processes is λ. Hence, all correlation lengths have to be at least of the order of magnitude of λ.

5. Renormalization group analysis

The results of section 4 are valid for small variances of $\log K$ (lowest order perturbation theory). In the following section, we extend the calculation to higher order perturbation theory by iterating the coarse graining procedure successively over small wave number bands.

Applying one coarse graining step we found the new mean coarse grained hydraulic conductivity value

$$\delta K_{ij}^{\mathrm{eff}}(\Lambda) = \int_{q',q''>\Lambda} \mathrm{d}^d q' \mathrm{d}^d q'' \overline{\widetilde{K}(-\mathbf{q}')\, \mathrm{i}q_i' G(\mathbf{q}', -\mathbf{q}'')\, \mathrm{i}q_j'' \widetilde{K}(\mathbf{q}'')}. \tag{33}$$

The wave numbers q', q'' are restricted to large wave numbers $> \Lambda$, here written in terms of limited integral ranges. The reason for doing so becomes obvious if we iterate the coarse graining process over small wave number bands. We obtain

$$\begin{aligned} &\delta K_{ij}^{\mathrm{eff}}(\Lambda - \delta\Lambda) \\ &\quad = \delta K_{ij}^{\mathrm{eff}}(\Lambda) + \int_{\Lambda-\delta\Lambda<q',q''}^{q',q''<\Lambda} \mathrm{d}^d q' \mathrm{d}^d q'' \overline{\widetilde{K}(-\mathbf{q}')\, \mathrm{i}q_i' G(\mathbf{q}', -\mathbf{q}'', \Lambda)\, \mathrm{i}q_j'' \widetilde{K}(\mathbf{q}'')}, \end{aligned} \tag{34}$$

where $G(\mathbf{q}', -\mathbf{q}'', \Lambda)$ is the respective Green's function of the Fourier transformed full head equation resulting from the former coarse graining step. Hence, (34) is still an implicit expression which requires further simplification for an analytical treatment by a closure procedure. A perturbation theory analysis offers one possibility and the explicit results of lowest order analysis we presented already in section 4. To improve this analysis, a resummation of perturbation theory contributions may be performed. In general, resummation techniques are quite problematic because they lead to a nonsystematic summation of perturbation theory contributions and a priori it is not evident whether the relevant contributions are taken into account. Fortunately, we can make use of exact results for the effective hydraulic conductivity in the limit of global upscaling (coarse graining to very large scales) in order to test the resummation procedure.

The simplest way to close the implicit expression (34) is to replace the Green's function by its coarse grained ensemble mean value

$$G(\mathbf{q}, -\mathbf{q}', \Lambda) \approx \frac{\delta(\mathbf{q}-\mathbf{q}')}{(\overline{K} + \delta K^{\mathrm{eff}}(\Lambda))\mathbf{q}^2} \tag{35}$$

and to perform the ensemble average in (34) over $\widetilde{K}$. This approximation is called renormalization of the Green's function. However, this approximation fails our test: it does not reproduce the geometric mean for the global upscaled (effective) hydraulic conductivity in isotropic media. A more detailed analysis reveals that a so-called vertex renormalization has to be taken into account. In this approximation, the lowest order fluctuating parts of the hydraulic conductivity are renormalized with the help of an expression which is related to the effective hydraulic conductivity. For further reference see also [9]. Therefore, we replace the lowest order fluctuating parts of the conductivities $\overline{K}\tilde{f}$ by

$$\overline{K}\tilde{f}\left(1 + \frac{\delta K^{\mathrm{eff}}(\Lambda)}{\overline{K}}\right). \tag{36}$$

Inserting both renormalization approximations (35) and (36) into (34) gives

$$\begin{aligned} &\delta K_{ij}^{\mathrm{eff}}(\Lambda - \delta\Lambda) \\ &\quad = \delta K_{ij}^{\mathrm{eff}}(\Lambda) + \int_{\Lambda-\delta\Lambda<q'<\Lambda} \mathrm{d}^d q'\, \overline{\tilde{f}(-\mathbf{q}')\tilde{f}(\mathbf{q}')}\, \frac{(\overline{K} + \delta K^{\mathrm{eff}}(\Lambda))\, \mathrm{i}q_i' \mathrm{i}q_j'}{\mathbf{q}'^2} \end{aligned} \tag{37}$$

which can be rewritten in the limit of $\delta\Lambda \to 0$ as a differential equation

$$\frac{\mathrm{d}\delta K^{\mathrm{eff}}(\Lambda)}{\mathrm{d}\Lambda}\delta_{ij} = -\left(\frac{1}{2\pi}\right)^d \Lambda^{d-1} \int_{q'=\Lambda} \mathrm{d}\Omega\, w(q' = \Lambda) \frac{(\overline{K} + \delta K^{\mathrm{eff}}(\Lambda))\, \mathrm{i}q_i' \mathrm{i}q_j'}{\mathbf{q}'^2}. \tag{38}$$

Here, we introduced spherical coordinates where $\mathrm{d}\Omega$ is an element of the solid angle. The integration is then performed over all angles while holding the radius fixed, $q' = \Lambda$. It results the isotropic hydraulic conductivity

$$\frac{\mathrm{d}\delta K^{\mathrm{eff}}(\Lambda)}{\mathrm{d}\Lambda} = -\left(\frac{1}{2\pi}\right)^{d} \Lambda^{d-1} w(k' = \Lambda)\big(\overline{K} + \delta K^{\mathrm{eff}}(\Lambda)\big)\frac{2\pi}{d}. \tag{39}$$

Equation (39) is called renormalization group equation. It can be solved analytically by separation of variables. We perform the integration of the right-hand side of (39) for consistency with our former results analogously as in section 4: the upper integration limit is modelled by the smooth Gaussian function (26).

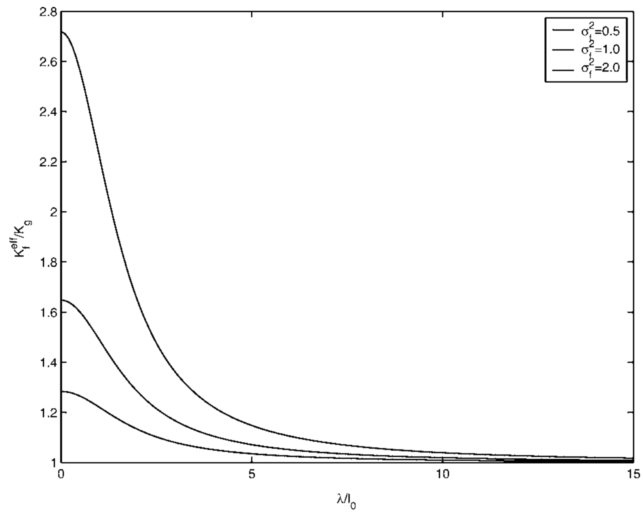

(a)

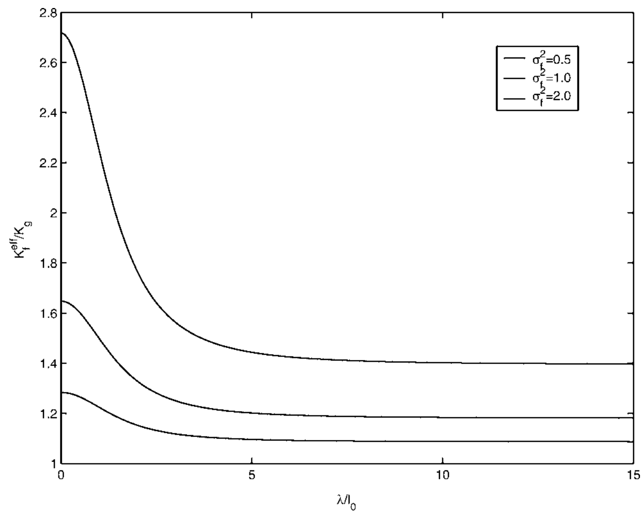

(b)

Figure 2. K^{eff}/K_g in two (a) and three (b) spatial dimensions for different σ_f^2.

Finally, we obtain

$$\ln\left(\frac{\overline{K} + \delta K^{\mathrm{eff}}(\Lambda)}{\overline{K}_f}\right) = -\frac{1}{d}\sigma_f^2\left(1 - \left(\frac{l_0^2}{l_0^2 + \lambda^2/4}\right)^{d/2}\right) \tag{40}$$

or after exponentiation

$$K^{\mathrm{eff}}(\lambda) = \overline{K}\exp\left(-\frac{1}{d}\sigma_f^2\left(1 - \left(\frac{l_0^2}{l_0^2 + \lambda^2/4}\right)^{d/2}\right)\right) \tag{41}$$

which is in lowest order perturbation theory equivalent to (28). The results are plotted in figure 2 for the cases of two and three spatial dimensions. We postpone the discussion of the results to a later section of the paper. However, the novelty of our results is that we give not only the spatially filtered head equation in its form (24) but also quantify the impact of subscale heteroegneities by the partially effective conductivity explicitly.

6. The numerical model

We study the quality of the results we presented in the last section in a two-dimensional numerical simulation. The aim of this investigation is to test whether the coarse-grained head equation (24) preserves essential physical features of the heterogeneous flow behavior.

It is evident that smoothing the head over the volume λ^d is equivalent to loosing information about the system: on coarser resolution scales, hydraulic conductivity contrasts tend to be smaller, head gradients are smoothed out and flow lines are straightened. However, the total amount of water flowing through the system has to be the same due to mass conservation of the fluid.

We generated a heterogeneous hydraulic conductivity field by using the numerical generator FGEN92 (for further reference see [29]). This field is considered in the following as our reference field. It represents the hydraulic conductivity field on the finest resolution scale. The hydraulic conductivity field is defined on a uniform rectangular grid of 256 by 256 quadratic cells. The uniform grid spacing is $\Delta x = \Delta y = 0.1$ m. Therefore, the whole spatial domain is $25.6 \cdot 25.6$ m^2. The hydraulic conductivity field is log-normally distributed in space as assumed in (2) and characterized by the following statistical properties: the variance of the $\log K$ is $\sigma_f^2 = 1$. The geometric mean of the hydraulic conductivity is chosen for simplicity as $K_g = 1$ m/d. The hydraulic conductivity values are spatially correlated and the correlation function is Gaussian as proposed in section 2. The correlation lengths are isotropic and given by $l_0 = 3$ m. In other words, one correlation length of the heterogeneous field is resolved by 30 grid cells. The whole domain contains 10 correlation lengths of the heterogeneous medium in each spatial direction. The heterogeneous hydraulic conductivity field is plotted in figure 3 together with the equivalent homogeneous hydraulic conductivity value that results from global upscaling in the limit $\lambda/l_0 \to \infty$. The latter is given by the geometric mean, formula (28).

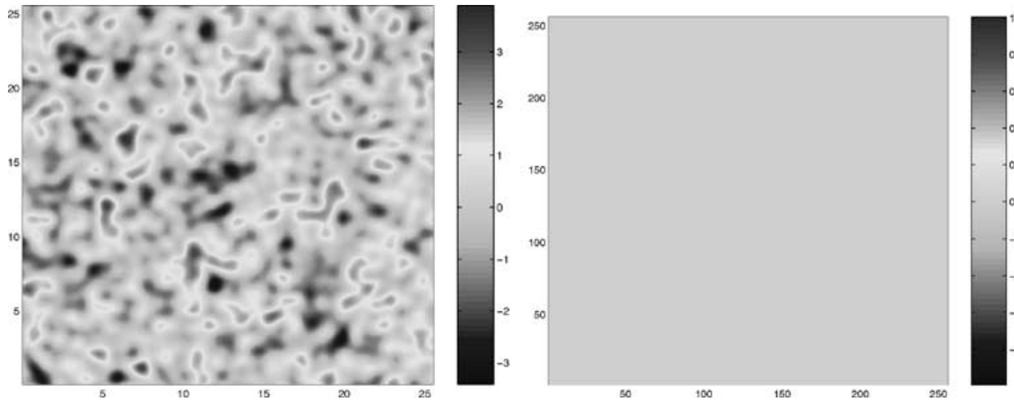

Figure 3. Heterogeneous fine-scale and equivalent homogeneous log-hydraulic conductivity field.

The local head equation (1) is solved by using the software MODFLOW (USGS) in the user shell PMWIN 5.1 by W.H. Chaing and W. Kinzelbach (1991–1999). For the flow simulation, we choose the following parameters: the rectangular domain is bounded by constant head boundaries at the inflow and outflow of the domain (located at the left and right boundaries). The mean head gradient aligned in x-direction is $\approx -10^{-2}$ with water flowing from the left to right. The numerical solver uses a preconditioned conjugate-gradient package with a modified incomplete Cholesky preconditioner.

The order of magnitude of the total water balance can be easily estimated. The whole domain contains 10 correlation lengths of the heterogeneous medium in each spatial direction. Therefore, the geometric mean approximates the equivalent homogeneous hydraulic conductivity reasonably well. With a mean head difference of $\Delta\phi = 2.5 \cdot 10^{-3}$ m over the whole domain and a geometric mean of $K_g = 1$ m/d, the total flow in m^2/d follows as

$$Q = K_g \Delta\phi = 2.5 \cdot 10^{-3}\ \mathrm{m}^2/\mathrm{d}. \tag{42}$$

Calculating the flux through the block numerically, we find the value of $Q = 2.44 \times 10^{-3}$ m^2/d which fits the theoretical value pretty well.

Moreover, we generate the coarser hydraulic conductivity fields. We explain the procedure in detail for one coarsening step. The next coarsening steps are analogous. The first slightly coarser grid has 128 by 128 cells such that 2 by 2 cells of the fine grid form one coarser grid cell. The mean hydraulic conductivity value on coarser grid resolution is given by formula (28) assuming a ratio of $\lambda/l_0 = 2\Delta x/(30\Delta x) = 2/30$. The simplest way to obtain the values $\langle \widetilde{K}(\mathbf{x})\rangle_\lambda$ is to average $\widetilde{K}(\mathbf{x})$ arithmetically over the 2 by 2 cells. We refer to this averaging procedure as block-averaging. In total, the coarser hydraulic conductivity field results as the sum of the two parts $K^{\mathrm{eff}}(\lambda) + \langle \widetilde{K}(\mathbf{x})\rangle_\lambda$. We subdivide each coarser grid cell in 2 by 2 subcells with identical hydraulic conductivity values which establishes again the 256 by 256 grid. For the next coarsening steps, we iterate the procedure until a single homogeneously distributed hydraulic conductivity value results. To that end, we have 7 coarsening steps to perform and get models with

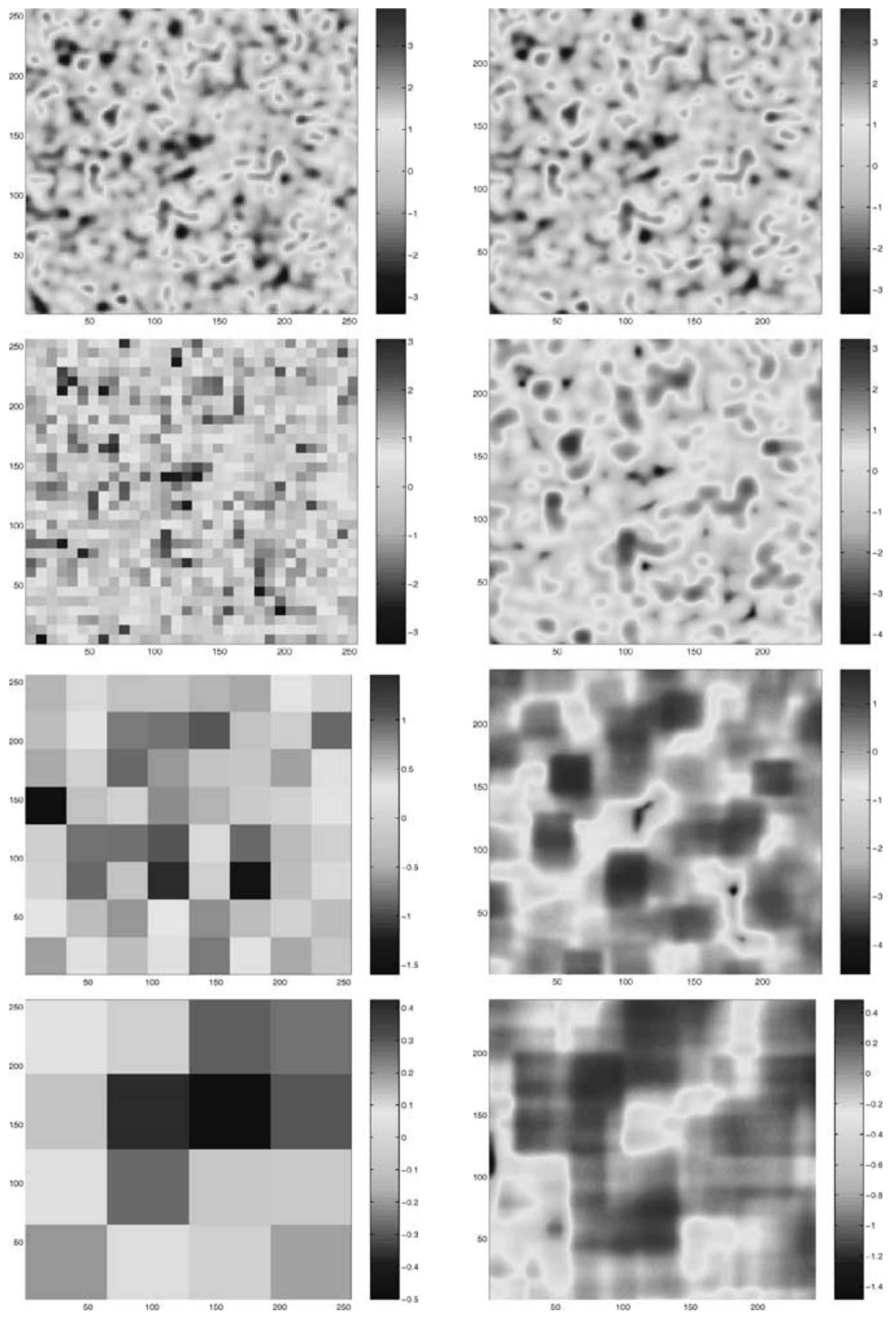

Figure 4. Coarse-grained hydraulic conductivity fields: block-averaged hydraulic conductivity fields in the left column (filter over 2×2, 8×8, 32×32, 64×64 cells) and moving-frame averaged hydraulic conductivity fields in the right column (filter over 34×34, 9×9, 27×27, 81×81 cells).

the resolution of 2^i by 2^i cells with $i = 1, \dots, 8$. Some of the coarse-grained hydraulic conductivity fields resulting from block-averaging are plotted on the left-hand side of figure 4.

After these preparative steps, the head equation is solved for each of the 7 coarser hydraulic conductivity fields. All numerical simulations are performed on the 256 by 256 grid providing comparable numerical results as far as possible. Moreover, the total flux is measured. The results are plotted in figure 4. As we can see the total flux values vary with a standard deviation of about 13% around the theoretical value.

The result can be improved by using an averaging procedure that is more related to the smoothing process introduced in section 3, equation (5). We call it moving-frame average. For this purpose, we slightly decrease the domain size to 243 by 243 grid cells. The moving-frame average over $\widetilde{K}(\mathbf{x})$ at location $\mathbf{x}$ follows as the arithmetic mean over the hydraulic conductivity values of all 8 next-neighbor cells plus the cell in the center (average over 3 by 3 cells). The average is performed at each location of the fine scale grid. It results in a coarser hydraulic conductivity field on 243 by 243 grid cells. Note that the average is performed on each grid cell individually. Therefore, the hydraulic conductivity field is smoothed but shows still small variations within the coarser grid block of the 9 cells. The procedure is iterated and 5 coarser hydraulic conductivity fields result with the resolution of 3^i by 3^i for $i = 1, \dots, 5$. Again, the head equation is solved on the coarser hydraulic conductivity fields and the total water flux is measured. Due to the small changes in the total domain size, the mean head difference is also smaller and the total water flux is approximately $Q \approx 2.4 \cdot 10^{-3}$ m^2/d. The total water balances are plotted for all numerical simulations in figure 5. In order to gain comparable results for the 256×256 realization and the 243×243 realization the total water flux of the 243×243 realization are scaled by the factor 2.5/2.4.

In general, the total water balances are better for moving-frame averaged hydraulic conductivity fields than for block-averaged hydraulic conductivity fields. They vary within a range of only 8%. Summarized, our numerical simulation demonstrated that the total water flux through the overall domain is conserved by the spatially filtered flow model within a tolerable standard deviation.

We compare our exact results with different ad-hoc averaging methods: the arithmetic mean over blocks, the geometric mean over blocks and the harmonic mean over blocks. For the arithemtic mean, we simply average the hydraulic conductivity over blocks of (2×2), (4×4), (8×8), (16×16), (32×32), (64×64) and (128×128) cells. For the harmonic mean, we average the inverse hydraulic conductivity over the same blocks and take the inverse afterwards. For the geometric mean, we perform the average blockwise over the logarithm of the hydraulic conductivity and exponentiate it. The comparison of all averaging methods is plotted in figure 6. It demonstrates that the best averaging method in a two-dimensional isotropic medium is the geometric mean over blocks and that our theoreticaly predicted effective hydraulic conductivities are in good agreement with this averaging method. However, our theoretical formalism also holds for three-dimensional domains. In a three-dimensional domain, the geometric mean fails and no ad-hoc averaging rule is known. It implies that our formalism is more general.

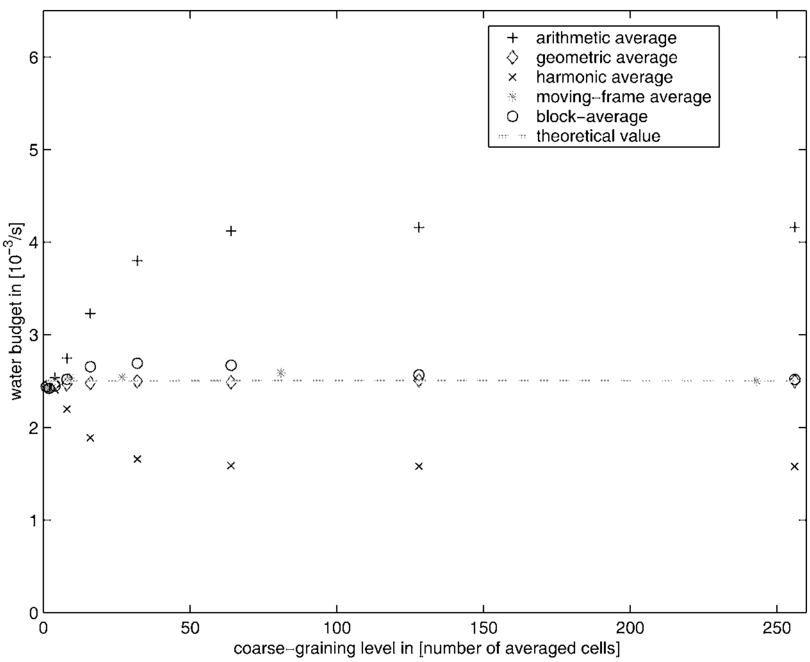

Figure 5. Total water budget for the different spatial averaging procedures at different coarse graining levels.

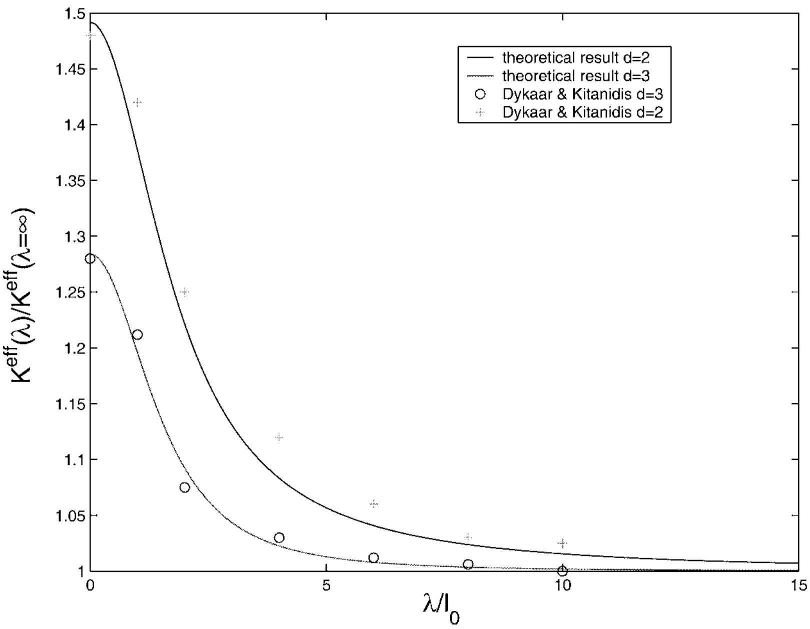

Figure 6. Analytical results for $K^{\mathrm{eff}}(\lambda)/K^{\mathrm{eff}}(\lambda = \infty)$ (solid lines) plotted against the ratio λ/l in two and three spatial dimensions, compared with numerical results of [13].

Moreover, it can extended to anisotropic media. In anisotropic media, no ad-hoc averaging rules are known either.

7. Discussion and conclusions

Using a coarse graining method we derived explicit results for the head equation on intermediate scales: small scale fluctuations in the heterogeneous conductivities are averaged out up to an arbitrary intermediate scale, whereas large scale fluctuations are still resolved by the coarse-grained model

$$-\nabla\big(\overline{K}+\big\langle\widetilde{K}(\mathbf{x})\big\rangle_\lambda\big)\nabla\big\langle\phi(\mathbf{x})\big\rangle_\lambda+\nabla\delta K^{\mathrm{eff}}(\lambda)\nabla\big\langle\phi(\mathbf{x})\big\rangle_\lambda=\big\langle\rho(\mathbf{x})\big\rangle_\lambda, \tag{43}$$

where $\langle\phi(\mathbf{x})\rangle_\lambda$ is the coarser head and $\overline{K(\mathbf{x})}+\langle\widetilde{K}(\mathbf{x})\rangle_\lambda\equiv\langle K(\mathbf{x})\rangle_\lambda$ is the coarser hydraulic conductivity field. Small scale fluctuations of the hydraulic conductivity field are averaged out, yet they show an impact on the coarse grained hydraulic conductivity represented by the additional term $\delta K^{\mathrm{eff}}(\lambda)$. We calculated $\delta K^{\mathrm{eff}}(\lambda)$ in lowest order perturbation theory and extended our results to higher order contributions by using a resummation technique (renormalisation group analysis). For isotropic media, we found the very compact result

$$K^{\mathrm{eff}}(\lambda)=\overline{K}\exp\left(-\frac{1}{d}\sigma_f^2\left(1-\left(\frac{l_0^2}{l_0^2+\lambda^2/4}\right)^{d/2}\right)\right). \tag{44}$$

Expression (44) models the scale-dependent transition from the arithmetic mean in case of no coarse graining to the effective conductivity for global upscaling. We tested our analytical result (44) also by numerical evaluation of (33) and found an excellent agreement of both results. For further reference, the reader is referred to [4].

The analytical results are comparable to results found by Dykaar and Kitanidis [13]. They calculated effective hydraulic conductivity values using a numerical spectral approach. In this approach, the effective hydraulic conductivity values are determined by a volume average over auxiliary functions which are defined as solutions of additional differential equations. Transforming their expressions for the effective hydraulic conductivity values into Fourier space equals our expression (23). However, Dykaar and Kitanidis [13] evaluate their expressions numerically using a spectral approach, whereas we obtain explicit results for the effective hydraulic conductivity value using a perturbation theory approach combined with a renormalization group analysis. The results which can be compared best are the numerical results plotted in figure 1 in [13] and our explicit results for a small variance of $\sigma_f^2=0.75$. For comparison, both results are plotted in figure 6. Numerical and explicit results fit well. Moreover, Dykaar and Kitanidis [13] also find in three dimensions the asymptotic effective hydraulic conductivity value of $K_g\exp(\sigma_f^2/6)$ for isotropic media. Again, they show numerical results whereas we present an analytical derivation of this result.

The results presented here are relevant with regard to different aspects in modeling ground water flow in heterogeneous formations.

First, the results can be used in order to separate spatialy variable hydraulic conductivities into large scale heterogeneous contributions modeled explicitly and small scale hydraulic conducitivities which are taken into account by a partialy effective hydraulic conductivity $\delta K^{\text{eff}}(\lambda)$. Modelling all spatial variability in detail implies a high computional effort which can even exceed the computational power of modern computers. Hence, a reduction of the grid block resolution, which is desired for numerical modelling purposes, can be performed without a big loss of information. The partial differential equation for the filtered head distribution, (43), can easily be discretized on a coarser grid with the corresponding hydraulic conductivity field $\langle K(\mathbf{x})\rangle_\lambda$. Moreover, the filtered head equation can be also used to reduce the computational effort solving the fine scale model in the framework of multi-grid methods. The idea is to improve the efficiency of multi-grid methods by a subtle choice of the coarse grid operators. It is applied in algebraic multi-level methods which show robustness and good convergence.

Second, taking into account small scale variabilities by coarse graining, intermediate scale variabilities can be modelled deterministically. The resolved-scale hydraulic conductivity field $\langle K(\mathbf{x})\rangle_\lambda$ can be estimated from local field tests. One could krige, e.g., the local field tests to yield a best estimate of the resolved-scale hydraulic conductivity. The best estimate tends to smooth the data. However, using the covariances of the kriged data we can account for the unobserved subscale variability. To that end, the covariances of the kriged data are to be used in (25) and in the renormalization group equation (39) instead of the filtered covariances of the unconditioned hydraulic conductivity field. Alternatively, one can proceed also in the following simpler way. The coarse-graining scale λ can be determined from the distance between the local field tests. Knowing λ, the subscale correlation length l_0 and the subscale variance σ_f^2 can be estimated using (32) and (31). Hence, all parameters are known in order to express $\delta K^{\text{eff}}(\lambda)$ and therefore to establish the model (43) explicitly.

Moreover, coarse graining provides a method to interprete measurement results obtained at different length scales or with a different spatial resolution. The data can be treated in form of a systematic post-processing. The data are transformed to a common scale and the information can be taken into account by a numerical model consistently. This point is also emphasized by Beckie [5] in a recent paper. He presents a comparison of methods for support volume determination. The filtering procedure used in the coarse graining procedure is one member of the family of spatial filtering concepts he proposes in equation (1).

References

[1] R. Ababou, D. McLaughlin, L.W. Gelhar and A.Thompson, Numerical simulation of three-dimensional saturated flow in randomly heterogeneous porous media, Transport Porous Media 4 (1989) 549–565.

[2] M. Abramowitz and I.A. Stegun, *Handbook of Mathematical Functions* (Dover, New York, 1965).

[3] F.G. Alabert, Constraining description of randomly heterogeneous reservoirs to head data: A Monte Carlo study, SPE paper 19600 presented at the 64th Annual Meeting, Soc. of Petr. Engrg., San Antonio, TX (1989).

[4] S. Attinger, J. Eberhard and N. Neuss, Filtering procedures for flow in heterogeneous porous media: Numerical results, Comput. Visualization Sci. 5(2) (2002) 67–72.

[5] R. Beckie, A comparison of methods to determine measurement support volumes, Water Resour. Res. 37(4) (2001) 925–936.

[6] R. Beckie, A.A. Aldama and E.F. Wood, Modeling the large-scale dynamics of saturated groundwater flow using spatial filtereing theory: 1. Theoretical development and 2. Numerical evaluation, Water Resour. Res. 32(5) (1996) 1269–1280 and 1281–1288.

[7] G. Dagan, *Flow and Transport on Porous Formations* (Springer, Berlin, 1989).

[8] D.S. Dean, I.T. Drummond and R.R. Horgan, Perturbation theory for effective diffusivity in random gradient flows, J. Phys. A Math. Gen. 28 (1995) 1235–1242.

[9] D.S. Dean, I.T. Drummond and R.R. Horgan, Effective diffiusivity in non-ositropic gradient flows, J. Phys. A Math. Gen. 28 (1995) 6013–6025.

[10] A. Desbarats, Spatial averaging of transmissivity in heterogeneous fields with flow toward a well, Water Resour. Res. 28(3) (1992) 757–767.

[11] C.V. Deutsch and A.G. Journel, Integrating well test derived effective absolute conductivities in geostatistical reservoir modeling, in: *Stochastic Modeling and Geostatistics: Principles, Methods and Case Studies*, eds. J. Yarus and R. Chambers, AAPG Computer Applications in Geology, No. 3 (Amer. Assoc. of Petrol. Geol., Tulsa, 1994) pp. 131–142.

[12] L.J. Durlovsky, Representation of grid block hydraulic conductivity in coarse scale models of randomly heterogeneous porous media, Water Resour. Res. 28(7) (1992) 1791–1800.

[13] B.B. Dykaar and P.K. Kitanidis, Determination of the effective hydraulic conductivity for heterogeneous porous media using a numerical spectral approach, 1. Methods and 2. Results, Water Resour. Res. 28(4) (1992) 1155–1178.

[14] Y. Efendiev, L.J. Durlofsky and S.H. Lee, Modeling of subgrid effects in coarse-scale simulations of transport in heterogeneous porous media, Water Resour. Res. 36(8) (2000) 2031–2041.

[15] Y. Efendiev, T.Y. Hou and X. Wu, Convergence of a nonconforming multiscale finite element method, SIAM J. Numer. Anal. 37(3) (2000) 888–910.

[16] L. Gelhar, Effects of hydrolic conductivity variations *n* groundwater flow, in: *Proc. of the 2nd Internat. Syposium on Stochastic Hydraulics*, International Association for Hydraulic Research, Lund, Sweden (Water Resources Publications, Fort Collins, 1977) pp. 409–428.

[17] L. Gelhar, *Stochastic Subsurface Hydrology* (Prentice-Hall, Englewood Cliffs, NJ, 1993).

[18] C.F. Harvey, Interpreting parameter estimates obtained from slug tests in heterogeneous aquifers, M.S. thesis, Appl. Earth Science Department, Stanford University, Stanford (1992).

[19] T.Y. Hou and X. Wu, A mulitscale finite element method for elliptic problems in composite materials and porous media, J. Comput. Phys. 134 (1997) 169–189.

[20] T.Y.H. Hou, X. Wu and Z. Cai, Convergence of a multiscale finite element method for elliptic problems with rapidly oscillating coefficients, Math. Comp. 68(227) (1999) 913–943.

[21] P. Indelman, A. Fiori and G. Dagan, Steady flow toward wells in heterogeneous formations: Mean head and equivalent conductivity, Water Resour. Res. 32(7) (1996) 1975–1983.

[22] A. Journel and C. Huijbregts, *Mining Geostatistics* (Academic Press, New York, 1978).

[23] W.D. McComb, *Physics of Fluid Turbulence* (Clarendon Press, Oxford, 1990).

[24] S. Neuman and S. Orr, Prediction of steady state flow in nonuniform geologic media by conditional moments: Exact nonlocal formalism, effective conductivities and weak approximation, Water Resour. Res. 29(2) (1993) 341–364.

[25] S. Nilsen and M. Espendal, Wavelet upscaling based on piecewise bilinear approximation of the hydraulic conductivity field, Transport in Porous Media (1996).

[26] D.S. Oliver, The averaging process in hydraulic conductivity estimation from well-test data, SPE Form Eval. 5 (1990) 319–324.

[27] G. Papanicolaou and S.R.S. Varadhan, Boundary value problems with rapidly oszillating random coefficients, Colloquia Mathematica Societatis Janos Bolyai (1979).

[28] F. Stauffer, Estimates of dispersion parameters by geostatistical methods – Laboratory and field applications, in: *Internat. Symposium – Contaminant Transport in Groundwater*, eds. H.E. Kobus and W. Kinzelbach, Stuttgart, 4–6 April 1989.

[29] M.J.L. Robin, A.L. Gutjahr, E.A. Sudicky and J.L. Wilson, Cross-correlated random field generation with the direct Fourier transform method, Water Resour. Res. 29(7) (1993) 2385–2397.

[30] Y. Rubin, A. Sun, R. Maxwell and A. Bellin, The concept of block-effective macrodispersivity and a unifierd approach for grid-scale and plume-scale-dependent transport, J. Fluid Mech. 395 (1999) 161–180.

[31] X. Sanchez-Vila, Radially convergent flow in heterogeneous porous media, Water Resour. Res. 33(7) (1997) 1633–1641.

[32] X. Sanchez-Vila, C. Axness and J. Carrera, Upscaling transmissivity under radially convergent flow in heterogeneous media, Water Resour. Res. 35(3) (1999) 613–621.

[33] E. Vanmarcke, *Random Fields: Analysis and Synthesis* (MIT Press, Cambridge, MA, 1983).

[34] S. Whitaker, *The Method of Volume Averaging*, Theory and Applications of Transport in Porous Media, Vol. 13 (Kluwer Academic, 1999).